EMERGENCY PROPULSION-BASED AUTOLAND SYSTEM

Nicolas Fezans*, Maxence Gamaleri*
***DLR (German Aerospace Center) - Institute of Flight Systems**
nicolas.fezans@dlr.de

Keywords: *Autoland, Propulsion-Controlled Aircraft, Emergency System, Monte Carlo Simulations*

Abstract

In this paper, an emergency autoland system capable of landing automatically with the ATTAS research aircraft only using engine thrust variations is presented. This autoland is intentionally kept as simple as possible, but demonstrates good performance even in the presence of uncertainties and external disturbances. The performance in the presence of wind shears is shown in the paper. It is based on a previously published propulsion-based control law for the inner loops. Implementing this simple emergency autoland in modern aircraft is not challenging. Aircraft already in service could also be retrofitted.

1 Introduction

Jet airplanes are usually designed to be controlled by means of both engines (mainly acting on speed/energy) and control surfaces which are deflected to generate aerodynamic forces and moments at several places on the airplane frame. These control surfaces are usually actuated by means of hydraulic actuators. Quite recently, electrical actuators have also been introduced in the most modern jet airplanes. As these systems are crucial for the control of the aircraft, simultaneous failures affecting them must be prevented. Therefore, aircraft control surface actuation systems are implemented using highly redundant architectures: multiple actuators, control signal transmission chains and power sources.

Even though aircraft are designed such that a complete failure of the primary control effectors is extremely improbable, this situation can still happen and has happened several times in the past (e.g. Japan Airlines flight 123 near Tokyo, United-Airlines flight 232 in Sioux-City or DHL in Bagdad). As shown in the three aforementioned accidents it might still be possible to control the aircraft by means of thrust variations. Of course the maneuverability of the aircraft is then very restricted, but this possibility has been investigated since the early 90's when a research program on propulsion controlled aircraft (PCA) took place at NASA. In this program, a pilot assistance system was developed and demonstrated in simulator as well as in flight tests with several aircraft types [1–3]. More recently developments have been made on PCA technologies at the DLR and a propulsion-based control law was even successfully demonstrated in flight test [4, 5]. The developed system was able to assist pilots and provide them good chances to land successfully. During the first part of our simulator studies, pilots did not receive explanations on the way they should use the system. The goal was to check experimentally the affordance of the developed system and how fast pilots were able to figure out how to use it. Results were very encouraging but it appeared that some of the airline pilots taking part to the studies misunderstood the basic flight dynamics principles the control law relies on, leading sometimes to dangerous reactions. After short explanations, all pilots were able to land with acceptable touchdown conditions in almost all following trials.

In our opinion, this good result reproduces the results obtained by NASA in the 90's but still is not fully satisfying. Indeed, both airline and military pilot trainings should not be used to train intensively for this very remote situation. Without specific training and without making pilot aware of the way aircraft can be controlled by means of thrust variations, the added value for the system is clear but much lower as it seems it could be. Apart from that, one of the results of the simulator tests was that the performance of pilots seemed to be mainly limited by the mental workload. This was not a surprise as the aircraft reaction is very slow and pilots must be extremely attentive to predict the consequences of their actions (even with the the assistance of the control law from [5]). This suggests a completely different solution: the design of an autopilot with an autoland function. This autoland permits to get results independently of pilot understandings of the way the system is working internally. Additionally, this will permit to get a performance level in the presence of disturbances that a human pilot would never obtain.

The autoland function of the autopilot will be presented in details in section 2. In section 3, the behaviour of the autoland is demonstrated using Monte Carlo simulations. Finally, conclusions and outlook are provided in section 4.

2 Propulsion-based autoland

For the design of the propulsion-based autopilot, two main options were considered:

- the design of a standalone autopilot, which would directly command the engines through the power lever angles,

or:

- the design of an autopilot as an outer loop for the pre-existing propulsion-based control law (see. [5]).

As it was estimated that the second option would ease significantly the development of the autopilot, this option was chosen. Of course, when imposing a structure to a controller the reachable performance and robustness might be reduced (compared to the unstructured case). It is later shown by simulation results that the performance level obtained is sufficient, which validates this initial choice.

The global structure can be represented by the block diagram in Fig. 1 in which the way the autopilot uses the already existing propulsion-based control law is explicitly shown. In this figure only the components of the autopilot that are activated during autoland operations are represented inside the “autopilot” block.

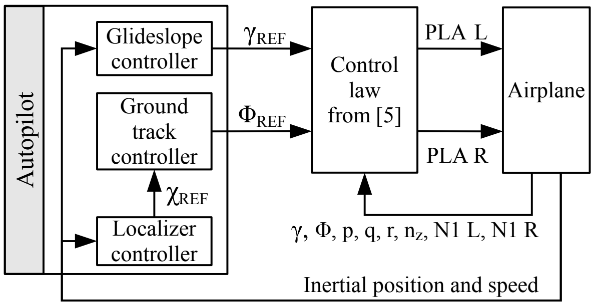

Fig. 1 Control structure for automatic landing

The autoland function has to intercept the runway centerline and the glidepath, to track them up to the ground and to land possibly with a flare. In a previous version of this autoland [6], the deviations with respect to the runway centerline and the glidepath were provided by the glideslope and localizer indicators. When the aircraft is quite far from the localizer and glideslope emitters, these indicators can be interpreted as an angular measurement of the lateral and vertical deviations. As shown in Fig. 1 and with the aim of giving more flexibility to the pilot to choose the approach slope and later to ease the definition and realisation of a flare maneuver, the classical ILS measurements were replaced by the inertial position and speed. Internally the reference system used is the WGS-84 system. Of course a relative positioning cannot be replaced by an absolute one without some other changes: in the present case it must be additionally assumed that the position and orientation of the runway are known with precision and that the absolute positioning is also precise enough. Note that “absolute positioning” does not mean GPS and only GPS, but could be obtained by coupling inertial platforms with GPS and barometric+radar altitude or any other useful source available.

2.1 The underlying control law of [5]

This autopilot is designed as an outer loop using the control law of [5], which is already following the references on the flight path angle and on the roll angle. In the current paper, this control law, how it works and how to tune it will not be re-explained in details but a short overview is presented hereafter.

2.1.1 *Control law requirements*

In this section, the main requirements for successful approach and landing by means of a PCA system are discussed with focus on how desirable they are, how difficult it will be to reach them, and which trade-off between the performance criteria should be made. Obviously, classical handling qualities criteria are not applicable for an aircraft having a propulsion-based control law.

Longitudinal Control

The longitudinal motion is mainly composed of the phugoid mode and the short-period mode. The period of the phugoid is generally between 30 and 60 seconds for transport airplanes. The frequency of the short-period mode depends on the aircraft and its center of gravity location, but would typically lie between 1.5 and 3 rad/s.

Increasing the total thrust of the engines leads to an increase of the energy rate of the aircraft. To really know the effect of this additional thrust on the movement of the aircraft, the pitch equation as well as the aerodynamics and mass characteristics of the aircraft must be known. For typical configurations, a simplified reasoning can be expressed as follows: a constant additional total thrust $\Delta T_t = \sum_i \Delta T_i > 0$ leads to a positive variation of the flight path angle γ and vice-versa, i.e. $\Delta T_i > 0 \Rightarrow \Delta\gamma(t \to \infty) > 0$ and $\Delta T_i < 0 \Rightarrow \Delta\gamma(t \to \infty) < 0$. This makes it possible to control the trajectory of the aircraft in the vertical plane.

With the typical frequencies and damping ratios of the short-period mode and of the phugoid as well as the typical dynamics of engines, no real challenge is expected in designing and tuning a control law assisting the pilots in the control of the flight path angle. Such a control law will basically consist of controlling the phugoid (acceptable response time, good damping, and no static error on the flight path) while avoiding unnecessary excitation of the short-period mode.

Note that the flight path angle cannot be controlled independently from the speed. In order to reach the runway the angle of descent (i.e. the flight path angle) must be controlled. Once the flight path angle is determined, there is no degree of freedom left to select the speed.

Lateral Control

The lateral dynamics of an aircraft are composed of:

- the Dutch roll mode exhibiting a pair of complex conjugate and stable poles with very low damping,
- the roll mode which is aperiodic and stable,
- the spiral mode which is slow and quite often slightly unstable.

As for the short-period mode, the Dutch roll mode and the roll mode are generally too fast to be significantly modified by means of the engines, in particular in the low-thrust domain that will generally be required for descent and approach. However, a control law based on thrust can easily modify the spiral mode in order to ease its control by a human pilot. For this, the coupling between yaw and roll is used: the pilot controls only the roll motion and the control law generates a yaw motion by means of asymmetric thrust allowing to get the induced roll corresponding to the pilot's commands. In previous studies PCA control laws were designed to follow a reference bank angle Φ_{REF} that was provided by the pilot. During the current research activities several other possibilities have been investigated in the ATTAS ground simulator. In particular a rate-command attitude-hold and a combination of roll rate and bank angle commands are being tested. They are both based on the control law presented hereafter: the difference is the way pilots provide the references to the system.

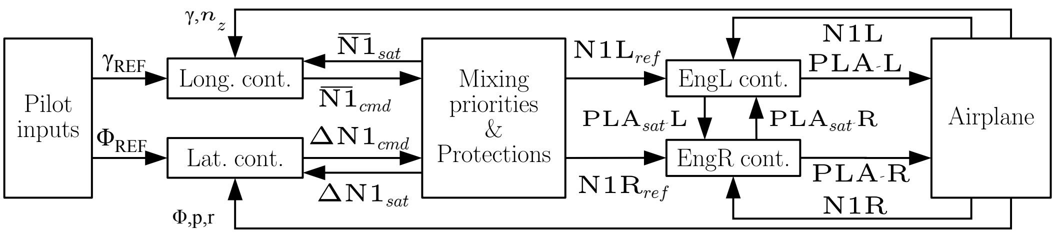

Fig. 2 Global architecture of the propulsion-based control law of [5]

Some reasonable goals for the lateral part of the control law are: to permit enough maneuverability, to reduce pilot workload by damping the lateral dynamics, and to ensure acceptable disturbance rejection without any action of the pilot.

2.1.2 Global architecture

The global architecture of this control law is presented in Fig. 2. It is based on a cascade control strategy with inner loops controlling the engines through commands in terms of Power Lever Angle (PLA) and outer loops controlling the longitudinal and lateral motions through symmetric and asymmetric thrust. The controllers in all these loops are based on simple PI or PID structures with feedforward terms and antiwindup. The inner loops have a crossfeeding in case of saturation (see signals $\mathrm{PLA}_{sat}\mathrm{L}$ and $\mathrm{PLA}_{sat}\mathrm{R}$ for antiwindup). A block labeled “Mixing priorities & Protections” connects the outer loops to the inner loops by allocating longitudinal ($\overline{\mathrm{N1}}_{cmd}$) and lateral ($\Delta\mathrm{N1}_{cmd}$) control actions to the two engines while satifying the limits for each engine. This leads to the two references $\mathrm{N1L}_{ref}$ and $\mathrm{N1R}_{ref}$ that are provided to the inner loops. Although this does not appear very explicitly in Fig. 2 the “Mixing priorities & Protections” block also connects the two outer loops by means of the antiwindup feedback signals $\overline{\mathrm{N1}}_{sat}$ and $\Delta\mathrm{N1}_{sat}$.

Further details on all the elements of this control law as well as on its tuning were already published in [5] and will not be reminded in the current paper. Results of both simulator and flight tests were included and illustrate that the control law follow the references on the flight path angle and on the roll angle well. The autoland system presented in this paper take the place of the pilot in the architecture of Fig. 2, as shown in Fig. 1.

2.2 Glideslope controller

The glideslope controller of the previous autoland version was based on the geometrical principle presented in Fig. 3, assuming that the glideslope indicator measurements can be converted approximately to a deviation angle e_{xz}. Contrary to what is shown in Fig. 3, with the usual ILS system the reference point would be at the glideslope emitter, i.e. along the runway shortly after the threshold. The position of the reference point shown in Fig. 3 is better as it permits to use the same approximation and to keep small deviation angles until touchdown. Small angles lead to an almost linear relationship between altitude error and deviation angle ($e_{xz} \approx 0 \Rightarrow \tan(e_{xz}) \approx e_{xz}$), which later simplifies slightly the tracking task. For practical reasons the real glideslope emitter cannot be placed under the runway as shown in this figure, but this is possible when defining a virtual reference point for the autoland system. Consequently, this reference point and the touchdown point are parameters which can be chosen by the pilot. The configuration shown in Fig. 3 with a reference point far behind the touchdown point and therefore under the runway is the one used later throughout the paper. Note that this does not represent the usual glideslope signal (same remark applies also for the e_{xy} later) and is only introduced here to defined the variable used in the description of the autoland outer loops. For gain scheduling purpose, the distance to the emitter or the runway is often used: if a virtual reference point far from the usual emitter position is chosen, the distance used for the gain scheduling must be corrected adequately.

The tracking of the rectilinear glidepath with

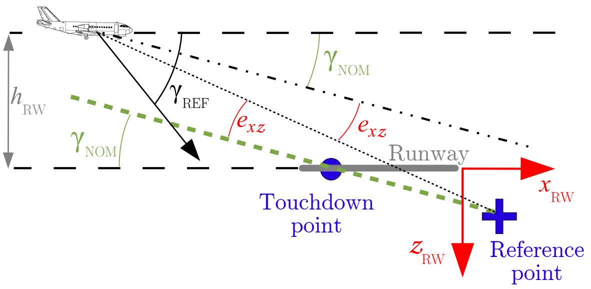

Fig. 3 Glideslope controller geometry definition

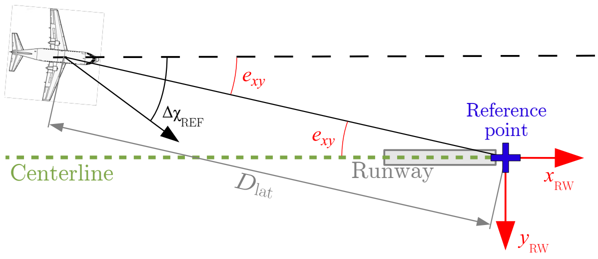

Fig. 4 Localizer controller

slope γ_{NOM} leading to the desired touchdown point (green dashed line in Fig. 3) is realised by means of a simple PID controller on the deviation angle e_{xz}:

$$\begin{aligned}\gamma_{REF} = \gamma_{NOM} + K_p(D_{lon})\ e_{xz} \dots \\ + K_i(D_{lon}) \int e_{xz} + K_d(D_{lon})\ \dot{e}_{xz}\ ,\end{aligned} \quad (1)$$

where D_{lon} is the distance used for the gain scheduling (usually the distance between the aircraft and the reference point). To prevent undesirable behaviour, this PID structure is completed with saturations and antiwindup (not detailed here but similar to the saturations and antiwindup shown in [5] for the inner loops). The time derivative $\dot{e}_{xz}$ of the deviation angle e_{xz} can be replaced by the expression obtained by differentiating analytical with respect to time (no need for numerical differentiation):

$$\dot{e}_{xz} = \frac{\dot{x}(h - h_{REF}) - \dot{h}(x - x_{REF})}{(x - x_{REF})^2 + (h - h_{REF})^2}\ . \quad (2)$$

2.3 Localizer controller

As shown in Fig. 4, the localizer controller uses the same principle as the glideslope controller. In most cases, there is no need to perform lateral maneuvers during the final part of the approach. The localizer emitter is usually placed behind the end of the runway. This position permits to provide a signal of good quality during the approach and on all positions on the runway. There is no need for selecting any other position for the reference point, therefore this position was used. The localizer controller works then exactly as the previous version, but uses a geometrically computed deviation angle signal. Note that it would be possible to use the e_{xz} signal previously defined for the glideslope controller and to use the real localizer indicator signal in the localizer controller.

The reference χ_{REF} provided by the localizer controller to the ground track controller is directly the sum of the runway direction and a correction angle $\Delta\chi_{REF}$ (see Fig. 4):

$$\chi_{REF} = \Psi_{RW} + \Delta\chi_{REF}\ , \quad (3)$$

with $\Delta\chi_{REF}$ being the output of a gain scheduled controller, having a PI structure:

$$\Delta\chi_{REF} = K_p(D_{lat}, s)\ e_{xy} + K_i(D_{lat}) \int e_{xy}\ , \quad (4)$$

but with $K_p(D_{lat}, s)$ a gain scheduled first order filter which is amplifying the high frequencies more than the low frequencies (lead-lag form). A similar effect could have been obtained using a derivative term based on $\dot{e}_{xy}$ (also analytically differentiable) combined with a first-order low-pass filter. In practice, there might be some reasons to use one or the other formulation: here the lead-lag form was simply used but this choice was not imposed by any specific constraint.

As for the glideslope controller, the scheduling compensate the increase of sensitivity of the deviation angle while approaching of the reference point. Only an approximated compensation was made but it is not required to keep the closed loop gain exactly constant all along the approach trajectory. The output of the localizer controller is a reference on the ground track, which is provided to the ground track controller whose role is to ensure that this ground track will be followed by the aircraft. The ground track controller is presented in the next section.

2.4 Ground track controller

The ground track controller generates a reference on the roll angle (which will be provided to the control law described in [5]) which permits to make the aircraft turn and therefore change the orientation of its ground trajectory. The lateral part of the autoland must ensure that this trajectory match the desired trajectory so that the aircraft will arrive at the chosen touchdown point.

The localizer controller (see previous section) generates a ground track reference that should permit to follow or rejoin the desired trajectory. The role of the ground track controller is then to make sure that this ground track reference will be followed.

The ground track controller consists of two modes which are combined in a "fuzzy-control way" for the transition between them:

- A mode used to perform small to large changes of ground track, which only consists in a highly nonlinear gain on the error e_χ between the reference and the current ground track. This part was kept unchanged between the regular ground track controller and this variation of it. In this mode the reference Φ_{REF} reads:
$$\Phi_{\text{REF}}[^\circ] = 10 \tanh\left(\frac{e_\chi[^\circ]}{10}\right) \quad . \qquad (5)$$
The hyperbolic tangent introduce a strong nonlinearity leading to a smooth saturation the generated Φ_{REF}. Extrema for Φ_{REF} are $\pm 10^\circ$ and are reached at $e_\chi \approx \pm 30^\circ$. This limitation to 10° commanded roll angle is quite restrictive but prevents entering in engaged turns without having the control authority that is required to come back to horizontal flight. The best value for this limit could be computed online, depending on the current damages of the aircraft. Here for simplicity only this 10° constant value was considered.

- A mode used for very small corrections, which after removing the integral term is basically a proportional controller ($K_p = 0.25$ for e_χ and Φ_{REF} in the same unit).

The transition between these two modes is made linearly for $|e_\chi| \in [0.2^\circ, 1.5^\circ]$, which lead to a nonlinear gain of 0.25 in the interval $[0.0^\circ, 0.2^\circ]$, progressively increasing to about 1 around $e_\chi = \pm 1.5^\circ$. In the intervals $\pm[1.5^\circ, (almost)30^\circ]$ the controller behaves as a linear proportional controller of gain 1.

This ground track controller is a simplified version of the one directly accessible to the pilot and with different gains. The pre-existing ground track controller could not be reused because a higher bandwidth was required in order to use it for centerline tracking in the presence of external disturbances.

3 Autoland evaluation

In this section the behaviour of the designed emergency propulsion-based autoland system is evaluated. Of course, with the same initial conditions, in the nominal case, and without disturbance the system lands systematically at the same position, speed, and attitude. In order to evaluate the usability of the system under more realistic conditions, the aircraft configuration must be varied (including mass, position of the centre of gravity, and possible structural damages). Influence of initial conditions and external disturbances must be analysed as well. In this paper, the results shown will focus on the behaviour in the presence of low altitude wind shears.

Although it is not shown in the paper, the influence of aircraft configuration as well as possible structural damages have also been investigated and the system was able to control the aircraft and land with all configurations and very strong damages. For instance the aircraft landed successfully with damages generating a roll torque corresponding to a fourth of the aileron roll authority at that speed. It is assumed that aircraft configuration cannot be changed, which means that the aircraft might not be in a configuration permitting to satisfy the usual operational requirements for landing (speed cannot be changed independently from the flight path angle). However, reaching the runway in some of the best conditions possible would still provide relatively good survival chances to people on board. Keeping the control of the aircraft and reaching the runway permits also to prevent additional deaths on ground.

3.1 Considered wind shears

3.1.1 Wind shear direction

When controlling the aircraft only by means of symmetric and asymmetric thrust variations the maneuverability is far from being as good as in the normal case. Moreover the number of degrees of freedom that a pilot can control is reduced: speed and flight path angle cannot be controlled separately. The same applies for sideslip and roll. With an aircraft satisfying the usual handling qualities criteria, the lateral component of wind shears presents a significantly lower risk than the longitudinal component of identical magnitude.

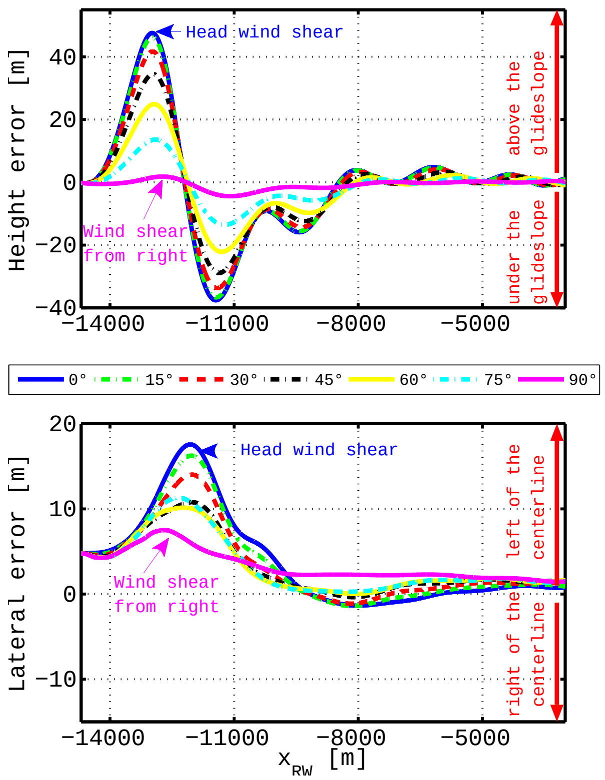

Fig. 5 Comparison between the deviations induced by wind shears of same magnitude ($\Delta W = 10$ m/s) but different directions

Although the lateral control of the aircraft is now significantly slower and less precise than for an aircraft with fully functioning primary control system, the performed simulations show that the deviations induced by lateral windshears is indeed still relatively small. This is illustrated with the simulations shown in Fig. 5, where the aircraft reactions to wind shears of the same magnitude but different directions are compared.

It should also be noticed that the lateral deviations caused by the purely longitudinal wind shear is higher than the lateral deviation caused by a purely lateral wind shear of same magnitude. With a perfectly symmetric aircraft, there will be no lateral deviation at all. However, no aircraft is perfectly symmetric and therefore a deviation will be observed. Note that the effect that is observed here does not correspond to strong asymmetry: to fly along a straight line (i.e. $\dot{\chi}_k = 0$) with all control surfaces to 0°, both a roll angle and a sideslip around 0.3° is required (imperfect lateral trim). These relatively small values are sufficient to generate the coupling shown in Fig. 5, where the head wind shear (blue line) generates the largest lateral deviations. Even stronger couplings should be expected with damaged aircraft.

3.1.2 Wind shear parameterised based on altitude or on time?

Physically, wind shears are differences of wind speeds and directions depending on the position considered (in 3 d.o.f.). Weather conditions evolve with time, which introduces the time as a fourth dimension in the description. When considering a specific landing on a specific runway at a specific time and with a specific approach path, all the wind possibilities in this 4-dimensional space will not be encountered: only the wind along the trajectory will affect the aircraft. Consequently, wind shears are often described in reduced forms. A typical form used to describe a wind shear is to define a wind speed and orientation depending only on the altitude. Note that in general wind shear related to microbursts cannot be reduced to a single dimension without losing too much information: microburst-induced wind shears are not considered in this paper.

When describing wind shears as a function of the altitude, it might be observed that the positive variation of winds in the direction of the aircraft speed (i.e. that causes initially a reduction of aircraft air speed) lead to stronger reactions than wind shears in the opposite direction. The reason for that is well-known: when the aircraft encounters this type of wind shear, it loses lift and begins to sink quicker, which lead to an even greater time-variation of the wind speed. Tail wind shears are thus amplified by the aircraft motion they induce, whereas head wind shears are attenuated by the induced aircraft motion.

During design phases it might be useful to consider time-based disturbances, but this rather artificial decoupling between aircraft motion and disturbance should be used with extreme caution when doing a performance assessment. In the following only altitude-based wind shears will be considered.

3.1.3 Wind shear distribution used

Due to the reasons given in the previous sections the following wind shear distribution was chosen:

- all wind shears are in the direction of the runway,
- all wind shears are single ramps based on altitude (see Fig. 6) with the parameters:
  - ΔW: uniform on $[-15\ ,\ +15]$ m/s,
  - H_{low}: uniform on $[10\ ,\ 310]$ m,
  - ΔH: uniform on $[10\ ,\ 210]$ m.

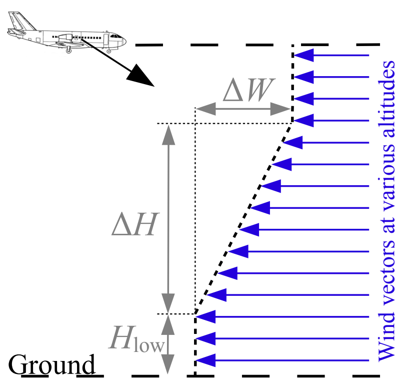

Fig. 6 Longitudinal single ramp wind shear

The sign and naming convention used hereafter is $\Delta W > 0$ if the variation of wind $\Delta\vec{W}$ goes in the direction of the flight (i.e. $\Delta\vec{W} \cdot \vec{x} > 0$). Therefore $\Delta W > 0$ will be called a tail wind shear and the opposite a head wind shear. Note that the definition of the tail wind shear is based on the sign of the wind variation and not on the wind direction itself!

3.2 Scenario and criteria

The considered scenario for all the Monte Carlo simulation results presented hereafter is the approach and landing at Hannover Airport (HAJ - EDDV) on runway 27R with the ATTAS (WFV-614) research aircraft. The simulation is always initialized with the aircraft at the coordinates 52.4235°N / 10.2806°E and an ASL altitude of 1000 metres. This initial position is located at 40 km from the runway threshold, left from the centerline and still outside the localizer reception zone. The initial course was chosen the same as the runway direction and the autoland will have first to turn right and then left to capture and hold the centerline direction.

Though not shown in the results that are presented later, this position as well as the flight direction at initialization were varied to verify no undesirable behaviour could be caused during switching from the regular autopilot modes to localizer capture and localizer hold. As these switches are working properly and the aircraft converge first to the given trajectory, this initialization does not impact the results obtained when encountering low-altitude wind shears. For this reason, the initialization conditions are not varied in the analyses presented hereafter.

Four criteria are used to assess the autoland performance

- $x_{RW}(t = TD)$: x-position of the touchdown point in the runway reference system (see red axes in Fig. 3 and 4) in x-direction,
- $y_{RW}(t = TD)$: y-position of the touchdown point in the runway reference system,
- $\Phi(t = TD)$: Roll angle at touchdown,
- $\dot{h}(t = TD)$: Sink rate at touchdown.

The first two criteria permit to check that the aircraft landed on the runway and not too far behind the runway threshold to permit to stop the aircraft. Ideally the aircraft will land at the chosen touchdown point. Landing outside the runway or too far behind the runway threshold is of course unacceptable regarding these criteria. Note that the limit after the threshold may be subject to many discussions: in particular the safety level associated to any value will strongly vary with the runway length and the current braking capabilities of the damaged aircraft. The value of 1250 metres behind the runway threshold was chosen.

The third criterion on the roll angle is a simplified version of a criteria aiming to prevent contact between the ground and the wings or the engines. No large roll angles were observed on the simulations and no problem is expected here, therefore there is no real need for a more exact computation. This criterion is kept to detect rapidly any deterioration: for instance a new tuning of the autoland gains could lead to excessively aggressive maneuvers in ground proximity, which is a behaviour which is dangerous, must be prevented, and could remain undetected at first if this criterion were not constantly monitored.

The last criterion permits to evaluate how hard the landing was and to verify that the structural limits of the airplane and the landing gears are not exceeded. The landing gears of the ATTAS are certified for a vertical impact velocity up to 700 ft/min and therefore this limit is taken for the landing acceptance criterion.

3.3 Results

When using the autoland based on the absolute position, the glidepath angle can be freely chosen and can thus be flat enough to avoid the necessity of performing a flare (assuming that the terrain around the chosen airport is flat enough). Considering the current speed of the aircraft a flight-path angle value that would lead to acceptable sink rate can be computed. This value is expected to be lower or equal to $-1.5°$ with typical values of transport airplanes. However, this simple reasoning do not take into account the effect of possible disturbances on the result and in particular it might be interesting to keep some margins and therefore to choose an even more gentle slope. If this is the case, how large should these margins be? In order to select the slope that offers the best chances for successful landing a detailed analysis must be performed.

The results obtained using the distribution described in section 3.1.3 for two different approach slopes are shown in Fig. 7. In all these simulations the autoland was set to follow a rectilinear slope until touchdown, i.e. without performing a flare. The upper-left plot in this figure represents the proportion of accepted landings (using the criteria mentioned in section 3.2) for each of the simulated approach slopes. The lower-left plot shows the respective proportions of unaccepted landings caused by tail and head wind shears. In the upper-right plot of this figure the maximum altitude at which a wind shear leading to an unaccepted landing started is represented for each slope and wind shear direction (tail or head). Finally in the lower-right part of this figure the respective proportions between the causes for nonacceptance are represented.

As no flare was performed, the acceptance of landings with the slope of $-2.9°$ is very low, which is logical as this slope leads to an excessive nominal sink rate. This acceptance increases significantly with the use of less steep slopes. As the nominal sink rate was already unacceptable for the $-2.9°$ slope, the results were almost identical for head and tail wind shears: with the most gentle approach slopes differences can be observed and tail wind shears are significantly more dangerous. At the same time, the risk of impacting the ground ahead of the runway threshold increases drastically when using more gentle slopes. This is mainly due to the initial loss of altitude that tail wind shears induce. Note that in the simulation environment “a perfectly flat airport neighbourhood” is assumed.

If the landscape around the airport permits to use a very gentle slope (between 0.4°and 1.2°) and if weather conditions indicates that wind shear (especially tail wind shear) encounters are

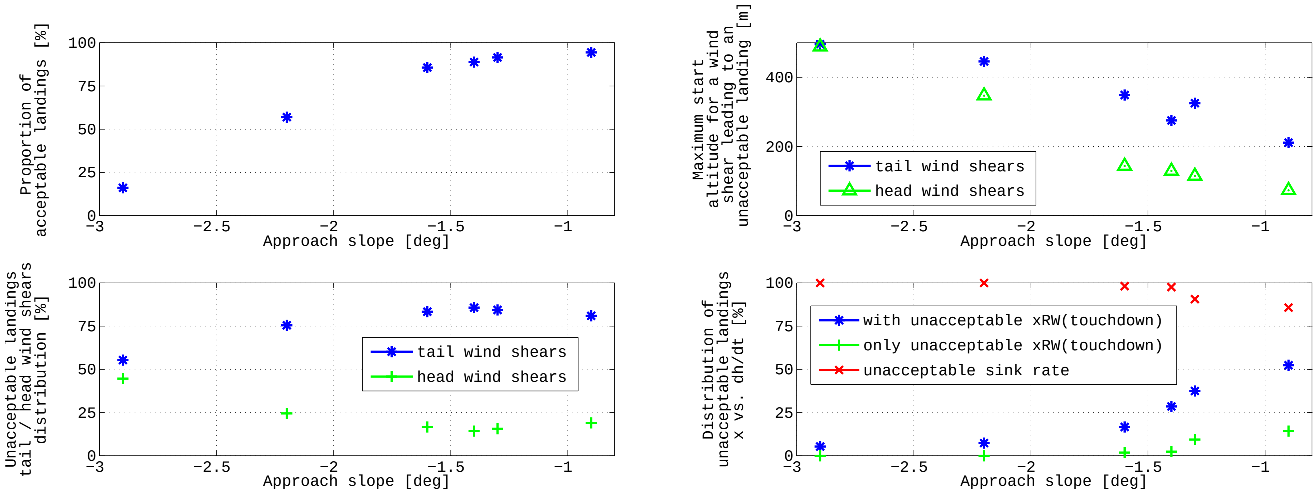

Fig. 7 Results obtained with various slopes

unlikely, this should be done. Pilots have access to the obstacles around the airports on the maps and can thus assess the risk related to the use of such a very gentle slope. This recommendation applies only to landings with the proposed autoland system: gentle slopes can lead to large variations of the touchdown position if the trajectory is not tracked well enough. This is likely to happen if the same trajectory is tracked manually.

If the weather is locally more uncertain, the first question is of course whether the situation is less uncertain on a different airport or runway: just as for the initial choice that the pilot would have made, the runway length, the safety equipments and expected hazard in case of runway excursion must be taken into account. If the runway is particularly long the risk of landing before the runway due to a tail wind shear could be partly alleviated by selecting a desired touchdown point quite far from the runway threshold. If this would not be the case, it seems at first better to make a quite hard landing at an acceptable position than a "soft" landing outside the runway or too far behind the threshold: most hard landings do not end up with deaths whereas quite a lot of runway excursions end tragically.

In order to compare the results obtained for various slopes, more specific simulations must be looked at. To explain the differences induced by varying the approach slope, two Monte Carlo simulations with less parameters were performed: one with the 1.6° slope and the other with the 2.9° slope. In both cases a tail wind shear ($\Delta W = 10$ m/s) was always considered but its position (and thus the encounter altitude) was varied. The results obtained are shown in Fig. 8. In the upper part of this figure each point represents the touchdown position in the runway coordinates: the red dot-dashed line around -3400 m represents the position of the threshold (above is ahead of the threshold). The points that correspond to the same slope are connected with lines in order to show how the the touchdown position varies with H_{low}. The lower part uses the same representation for the sink rate $\dot{H}$ at touchdown: the red dot-dashed line is the certified value for the landing gears of the ATTAS.

In this figure, the curves for x at touchdown oscillate with different periods. This is a consequence of the excitation of the phugoid mode by the wind shear: the resulting oscillation is superimposed to the "ideal path" and leads to variations of the touchdown positions depending on the altitude where it was initiated. These curves are discontinuous because there are limit cases leading to land at one oscillation if the wind shear occurred at a given altitude, but at the previous one if the wind shear occurred at an only slightly lower altitude. These discontinuities on the x position correspond to peaks on the curves of $\dot{H}$ that go to 0 (or slightly lower as the limit case was not perfectly found in the simulations made). Looking at such curves, it is obvious that consolidated values (e.g. mean, standard deviations, quantiles,

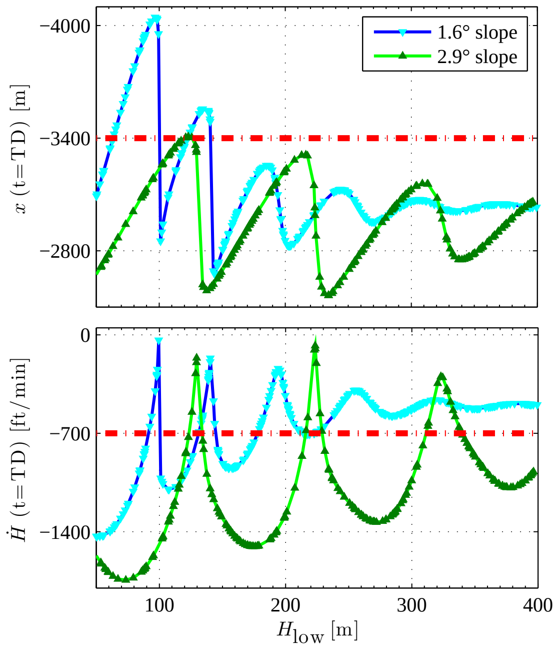

Fig. 8 Variations of touchdown positions for the same tail wind shear (10 m/s) depending on the encounter altitude.

etc.) must be taken with precaution as their dependence to the input distributions used is very strong. This applies of course also to the results shown in Fig. 7.

In this figure the oscillations shown have different periods. Reason for that is that the time required to reach the ground from the time the wind shear is encountered is approximately the quotient of the encounter altitude by the sink rate: therefore for a given encounter altitude the more gentle the slope is the more time is available to restabilise the aircraft on the ideal slope. This explains why the oscillation vanishes "earlier" (i.e. at lower encounter altitudes) for the 1.6° sloper than for the 2.9° slope. The fact more gentle slopes leads to higher risk to reach the ground before the runway is also clearly visible in this figure. The mean x-touchdown value during the "first" two oscillations with the 1.6° slope deviates clearly from the -3000 m value set for the ideal touchdown point, which is not the case for the 2.9° slope.

When looking at the proportion of acceptable landings (Fig. 7), the values even for relatively flat approaches are around 80 - 90%, which still seems quite far from the $100\% - \varepsilon$ that one would like to get. It should be kept in mind that the aircraft is assumed to have lost control of its control surfaces which is rather unlikely to happen. This aircraft is controlled only by means of its engines thanks to an emergency assistance system. In addition to this already very critical scenario, low altitude wind shears are encountered during the approach. Under these conditions the performance reached is already very good. Beside, the implementation of this emergency system do not required specific hardware: it could run on the currently existing flight computers and even be integrated in a software update of the system already flying.

Taking the airspeed measurement into account, the wind shear could be explicitly detected and precompensated. This would alleviate the initial reaction of the aircraft, but not completely cancel it. Indeed, there is no possibility to distribute the aircraft energy among kinetic and potential energy (usually possible through the horizontal trim and the elevators), which would be required to get an even more efficient alleviation of the wind shear. We only can compensate energy deficits or excesses.

Though not desirable, hard landings are often not fatal. Landing before the runway seems more critical, but if the weather is uncertain and there was no derouting possible, the most praticable solution would be to choose a touchdown point further on the runway (here it was chosen only 400 m behind the runway threshold) which would significantly reduce this risk.

4 Conclusions and outlook

An emergency propulsion-based autoland system for the ATTAS (VFW-614) research aircraft was presented. It consist in a simple outer loop to a control law previously published by the authors [5]. The performances of the complete system were shown in the paper with a focus on disturbance rejection capabilities. Various additional developments have already been made and tested in desktop simulation, which includes: curved trajectory tracking, flare maneuvres, and a feedforward that is activated only for strong disturbances. These systems are still being developed, but already improve the good performance of the emergency propulsion-based autoland system. It is also planned to port this autoland (and underlying control law) for the DLR A320 ATRA research aircraft and at least to test it in a simulator.

The proposed system provides very good survivability chances and in most cases no hull loss should even be expected, though the failure condition leading to the use of this system is currently classified as “catastrophic”. A typical issue encountered when introducing a new emergency system in addition to the existing ones is related to the possible activation of this system when not required. In the case of the emergency propulsion-based autoland system proposed in this paper, this issue is easy to address as it is very easy to know with certainty whether primary control systems are still working or not. Only if none of them is working the system can be used. The readiness level of this technology is high enough to implement it in flight control systems and the associated costs are very low (basically a couple of additional modes in flight control softwares). To our mind, assuming that the pursued flight safety strategy follows the “As Low As Reasonably Practicable” (ALARP) precept: it seems there is no good reason for not introducing this emergency system (or any suitable alternative) in transport aircraft. Besides, the costs assosiated with a single accident (investigation, legal procedures, possible responsabilities, image loss etc.) are expected to be significantly higher than the development costs of this additional and nonmandatory function for a complete family of modern fly-by-wire airplanes.

References

[1] Burcham, F. W. Jr., Burken, J. J., Maine, T. A. and Fullerton, C. G., *Development and flight test of an emergency flight control system using only engine thrust on an MD-11 transport airplane*. NASA/TP-97-206217, 1997.

[2] Burcham, F. W. Jr., Maine, T. A., Fullerton, C. G. and Webb, L. D., *Development and flight evaluation of an emergency digital flight control system using only engine thrust on an F-15 airplane*. NASA/TP-3627, 1997.

[3] Bull, J., Mah, R., Hardy, G., Sullivan, B., Jones, J., Williams, D., Soukup, P., Winters, J., *Piloted simulation tests of propulsion control as backup to loss of primary flight control for a B747-400 jet transport*. NASA/TM-112191, 1997.

[4] de Almeida, F., *Trajectory tracking with fault-tolerant flight control system: a model predictive approach*. PhD thesis TU Braunschweig, ISBN: 978-3-8322-8546-3, 2009.

[5] Fezans, N., Simple control law structure for the control of airplanes by means of their engines. *in Advances in Aerospace Guidance, Navigation and Control*, Ed. F. Holzapfel and S. Theil, Springer, ISBN 978-3-642-19816-8, 2011.

[6] Fezans, N. and Kappenberger, C., Approaches and vista on flight control systems reconfiguration - motivating example: aircraft control by means of engine thrust. *ONERA-DLR Aerospace Symposium*, Toulouse, France, 2011.

[7] de Almeida, F., Waypoint navigation using constrained infinite horizon model predictive control, AIAA-2008-6462. *AIAA GNC*, Honolulu, HI, USA, 2008.

[8] de Almeida, F. and Leißling, D., Fault-tolerant model predictive control with flight test results, *Journal of Guidance, Control, and Dynamics*, 0731-5090, Vol. 33 No. 2, 2010.

[9] Proctor, F. H., Hinton, D. A., Bowles, R. L., A windshear hazard index, Paper: 7.7, *9th Conference on Aviation, Range and Aerospace Meteorology*, Orlando, FL, USA, 2000.

Copyright Statement